Bluetooth Interference Suppression in IEEE 802.11b

Erik Björnemo
Signals and Systems Group, Uppsala University[1]
Box 528, SE-751 20, Uppsala, Sweden
eb@signal.uu.se

***Abstract*— We study the coexistence of IEEE 802.11b and Bluetooth, and more specifically the performance gains obtained using a frequency domain Bluetooth interference suppression scheme at the IEEE 802.11b physical layer. Focus is on the reduction of packet error rates in heavily interfered environments.**

The frequency domain structure of the signals is utilised to separate multiple interferers, thereby simplifying the frequency domain suppression. We develop a minimum mean square optimal suppression method for batch-wise processing of baseband data, and a reduced complexity sub-optimal implementation. The latter turns out to be equivalent to a Wiener smoother based on estimated signal energies.

Simulations indicate that the Wiener based smoother drastically reduces the packet error rate in interfered transmissions, especially for the lower transmission rates. The gains are substantial for single as well as multiple interferers.

1 Introduction

As the license exempt use of the 2.4 GHz band increases, so does the need for communication systems to efficiently handle interference. Several theoretical and empirical studies concerning coexistence of IEEE 802.11b and Bluetooth have been published, showing that substantial performance losses may be caused in both systems (see for example [1] and [2]). In this paper we investigate the suppression of Bluetooth interference in an IEEE 802.11b receiver. We propose a method which tracks and suppresses the interfering Bluetooth signals at the IEEE 802.11b physical layer.

Previously proposed coexistence approaches include collaborative methods for interference avoidance by coordination of Bluetooth and IEEE 802.11b packet transmissions. While effective, these coordinated actions require collocated systems, or changes in the standards, to enable inter system communication. Also non-collaborative solutions aimed at interference avoidance have been investigated. Typically, they adapt packet scheduling – in time or frequency – based on measured channel quality [3]. An adaptive frequency hopping scheme of this kind was recently adopted in the Bluetooth specification [4].

A complement to interference avoidance is interference suppression at the physical layer, which is the approach we adopt in this work. In [5], a recursive least squares filter is used to remove Bluetooth signals from IEEE 802.11b baseband data. It is shown to perform well for the 1 Mbit/s rate with only one interferer, but performs worse for the 11 Mbit/s rate and fails to handle more than one interferer.

2 Overall Goal and Proposed Approach

We consider an IEEE 802.11b device in receive mode. The aim is a non-collaborative, physical layer method that relies on received baseband data only, and does not impose any changes in the Bluetooth or IEEE 802.11b standards. The overall goal is to minimise the packet error rate. We pursue this goal indirectly by minimising the mean square error in the data.

The suppression algorithm handles multiple simultaneous interferers, and we use the following frequency domain structure of the signals to simplify this. First, compared to the bandwidth of the IEEE 802.11b receiver, roughly 22 MHz, Bluetooth signals are narrow-band and cover approximately 1 MHz. Second, the Bluetooth transmitters hop between 79 known carrier frequencies, spaced 1 MHz apart. We therefore apply the fast Fourier transform (FFT) as an efficient method for separation of simultaneous interferers present within the receiver bandwidth. The FFT approach implies batch-wise processing of data, which in turn introduces a delay. This delay, and the tracking of hopping interferers, require the batches to be much shorter than the IEEE 802.11b packet length.

In summary, we batch-wise minimise the mean square error in discrete Fourier transformed baseband data, with the goal of minimising the packet error rate.

3 Signal Models and Parameter Uncertainties

In this section we present our models of the signals, along with all relevant prior information I about their parameters. Based on these models and the parameter uncertainties, we assign the probability distributions relevant to the suppression scheme. We will throughout this paper use probability theory as extended logic, thus using it to do plausible reasoning based on our state of knowledge. The product and sum rules of probability theory constitute the only internally consistent way of reasoning under uncertainty, and they process our incomplete information with full efficiency. All prior probabilities are assigned using transformation groups and the principle of maximum entropy (MaxEnt) [6].

In our model of the received baseband data r_n, we include the IEEE 802.11b signal s_n, thermal noise v_n, and Bluetooth interferers $x_{m,n}$, where n denotes the sample number and m the channel number. Sampling is at 802.11b symbol rate. We model the frequency domain data as

$$R_k = S_k + \sum_{m=1}^{M} X_{mk} + V_k, \qquad (1)$$

where $k = 0, 1, \ldots, N-1$ is the frequency bin number, N is the batch size and M is the number of non-overlapping Bluetooth channels within the receiver bandwidth. We use the subscript mk when bin k is within channel m. All

[1]This work was partly funded by the graduate school PCC++.

propagation channels are modelled as slowly flat fading, i.e. as a constant attenuation over each batch.

3.1 IEEE 802.11b

These systems use differential BPSK or QPSK combined with a spreading sequence or complementary codes [7]. Assuming perfect symbol synchronisation and no inter symbol interference, we use the received transformed signal model

$$S_k = \frac{\sqrt{E_s}}{\sqrt{N}} e^{j\theta_s} \sum_{n=0}^{N-1} C_n e^{-j2\pi\frac{kn}{N}} \quad (2)$$

where $\sqrt{E_s} e^{j\theta_s} C_n = s_n$. Here, E_s is the received energy per symbol, θ_s is a phase rotation, and C_n are the transmitted complex symbols.

- E_s At the start of the reception, the energy is unknown but bounded. From above by regulations and receiver efficiency, and from below by the sensitivity of the receiver. Since E_s is a scale parameter, this uncertainty prescribes $p(E_s|I) \propto 1/E_s$ over $[E_{s-}, E_{s+}]$.
- θ_s The differential demodulator does not track absolute phase, and therefore θ_s is unknown. We assign a uniform distribution $p(\theta_s|I)$ over $[0, 2\pi]$.
- C_n The received symbols are from the alphabet $\{\exp(j(1/2 + d)\pi/2)\}$, where d is the encoded unknown transmitted information (BPSK: $d = 0, 2$ QPSK: $d = 0, 1, 2, 3$). All symbols are independently equally probable.

We conclude from (2) that, given E_s, all S_k are uncorrelated and have probability distributions $p(S_k|E_s I)$ with zero mean and variance E_s. By virtue of the central limit theorem these distributions are Gaussian for large N, and independent.

3.2 Bluetooth

A Bluetooth signal is well described as a continuously phase modulated signal [4], and its transform is

$$X_{mk} = \frac{\sqrt{E_m}}{\sqrt{N}} e^{j\theta_m} \sum_{n=0}^{N-1} e^{j\phi(nT_s - t_o, \mathbf{Y}) - j2\pi\left(f_m T_s + \frac{k}{N}\right)n}. \quad (3)$$

Here, E_m is the received energy per receiver sample, $\phi(t, \mathbf{Y})$ is the continuous phase modulation of the binary information sequence $\mathbf{Y}$ (modulation index h, GMSK pulse of bandwidth 0.5 MHz), f_m is the frequency offset between the receiver's and interferer's carriers, t_0 is the timing offset, θ_m is the phase difference, and T_s is the receiver sampling time:

- E_m Bounded in the same manner as E_s, provided an interferer actually is present. Assign $p(E_m|B_m I) \propto 1/E_m$ over $[E_{xmin}, E_{xmax}]$, where B_m denotes interferer presence in channel m.
- θ_m Unknown: $p(\theta_m|I)$ is uniform over $[0, 2\pi]$.
- t_0 Unknown, but maximally one Bluetooth bit period: $p(t_0|I)$ is uniform over $[0, 1]$ μs.
- $\mathbf{Y}$ Unknown information sequence: ± 1 equally probable.
- f_m The allowed deviation according to the Bluetooth specification is roughly ± 100 kHz. We assign a uniform distribution $p(f_m|I)$ over this range.
- h Required to be within $[0.28, 0.35]$, over which $p(h|I)$ is uniform.

We treat the parameters E_m and θ_m analytically, while resorting to numeric calculations for the others. We do this by computing the variance σ^2_{mk} for $p(X_{mk}|E_m \theta_m I)$ using Monte Carlo simulation of (3). The uniform $p(\theta|I)$ assures further that $p(X_{mk}|E_m I)$ has zero mean. Now, by use of only the mean and variance as prior information, this latter probability distribution is Gaussian according to the maximum entropy principle. The numerical procedure is an approximate marginalisation over the nuisance parameters t_0, $\mathbf{Y}$, f_m and h. In this way we include our initial uncertainty about their values in $p(X_{mk}|E_m I)$, but we have also permanently removed them from subsequent calculations. This simplification of our model in (3) will degrade the suppression performance, but we believe that it is a very small degradation, especially compared to the reduction in complexity.

3.3 Thermal Noise

The noise power is assumed to be known with good accuracy. We assign a Gaussian zero mean probability distribution $p(V_k|I)$ with variance E_v corresponding to the noise power.

3.4 Interferer Presence

Let B stand for Bluetooth presence within the receiver's range, and let $\overline{B}$ stand for an interference free situation. Denote the presence of exactly i interferers B^i. We make a conservative probability assignment $P(B|I) = P(\overline{B}|I) = 0.5$ based on the fact that we do not know in which type of environment – heavily disturbed or undisturbed – the IEEE 802.11b receiver is operating. Furthermore, Bluetooth networks operate independently of each other, so we assign independent probabilities $P(B^i|I) = P(B^1|I)^i$ for $i \geq 1$. In summary, we get

$$P(B^i|I) = \begin{cases} \frac{1}{2} & , \quad i = 0 \\ \left(\frac{1}{3}\right)^i & , \quad i > 0 \end{cases} . \quad (4)$$

There are $L = 79$ Bluetooth channels, which leads to $P(B_m|B^i I) = 1 - (78/79)^i$. Marginalisation over B^i gives

$$P(B_m|I) = \frac{P(B^1|I)}{1 - P(B^1|I)} - \frac{(L-1)P(B^1|I)}{L - (L-1)P(B^1|I)}, \quad (5)$$

which numerically is $P(B_m|I) = 1/106$.

4 Optimal Interference Suppression Scheme

Our goal is to make a minimum mean square estimate of $\{s_n\}$ for each batch $\{r_n\}$ in order to reduce the packet error rate. This estimate is given by the mean value of the probability distribution $p(\{s_n\}|DI)$, where D denotes the batch of data. An equivalent procedure is to find the mean of $p(\{S_k\}|DI)$ for the frequency domain data. For brevity, let E denote E_s, $\{E_m\}$ and E_v collectively. Then

$$p(\{S_k\}|DI) = \int p(\{S_k\}|EDI) p(E|DI) \mathrm{d}E \quad (6)$$

in which

$$p(\{S_k\}|EDI) = \prod_k p(S_k|EDI). \quad (7)$$

Proceeding with the individual distributions for S_k and Bayes' theorem, we get

$$\begin{aligned} p(S_k|EDI) &= p(S_k|R_kEI) \\ &= \frac{p(R_k|S_kEI)p(S_k|EI)}{p(R_k|EI)}. \end{aligned} \quad (8)$$

All distributions on the right hand side in (8) are Gaussian: $p(R_k|S_kEI)$ has mean S_k and variance $E_m\sigma^2_{mk}+E_v$; $p(S_k|EI)$ has zero mean and variance E_s; $p(R_k|EI)$ has zero mean and variance $E_s+E_m\sigma^2_{mk}+E_v$. It can be shown that

$$\langle S_k|EDI\rangle = \frac{E_s}{E_s+E_m\sigma^2_{mk}+E_v}R_k. \quad (9)$$

Insertion of (9) in (6) leads to the minimum mean square estimate

$$\langle S_k|DI\rangle = R_k\int\frac{E_s}{E_s+E_m\sigma^2_{mk}+E_v}p(E|DI)\mathrm{d}E. \quad (10)$$

This is a marginalisation over uncertain energies in a Wiener smoother – weighting the smoother for each set of energies with their respective probability density gives the optimal result.

The evaluation of $p(E|DI)$ in (10) does not lead to a closed-form solution. We work out everything needed for the implementation of a suppression scheme, but leave some details out due to space limitations. Let D_m denote data from channel m, and let E_{sv} denote E_s and E_v collectively. The posterior probability for E is

$$\begin{aligned} p(E|DI) &= p(\{E_m\}|E_{sv}DI)p(E_{sv}|DI) \\ &= p(E_{sv}|DI)\prod_m p(E_m|E_{sv}D_mI). \end{aligned} \quad (11)$$

We proceed by studying $p(E_m|E_{sv}D_mI)$ and $p(E_{sv}|DI)$ separately. The posterior probability distribution for E_m depends on the probability for B_m:

$$\begin{aligned} p(E_m|E_{sv}D_mI) &= p(E_m|B_mE_{sv}D_mI)P(B_m|E_{sv}D_mI) \\ &\quad +\delta(E_m)P(\overline{B}_m|E_{sv}D_mI) \end{aligned} \quad (12)$$

where

$$p(E_m|B_mE_{sv}D_mI)\propto p(D_m|B_mE_mE_{sv}I)p(E_m|B_mI) \quad (13)$$

and

$$\frac{P(B_m|E_{sv}D_mI)}{P(\overline{B}_m|E_{sv}D_mI)} = \frac{P(B_m|I)\int p(D_m|B_mE_mE_{sv}I)p(E_m|B_mI)\mathrm{d}E_m}{P(\overline{B}_m|I)p(D_m|\overline{B}_mE_mE_{sv}I)p(E_m|\overline{B}_mI)}. \quad (14)$$

The posterior for E_{sv} depends on the probability for B^i as

$$\begin{aligned} p(E_{sv}|DI) &\propto p(D|E_{sv}I)p(E_{sv}|I) \\ &= p(E_{sv}|I)\sum_i p(D|B^iE_{sv}I)P(B^i|I). \end{aligned} \quad (15)$$

All the terms in the sum in (15) are straightforward to find by application of the product and sum rules of probability theory, but are not displayed here. Except for this last part, we have now broken up $p(E|DI)$ into already quantified probabilities and probability distributions. Inserting them in (10), we have the mean square optimal solution. Unfortunately, there is no analytically tractable solution. The optimal scheme is however the basis for the approximate solution we develop in the next section, and could be implemented numerically provided enough computing power is available.

5 Reduced Complexity Implementation

We consider the complexity of a direct numerical implementation of the optimal scheme prohibitive. This is mainly due to the marginalisation over E and B^i in (10) and (15). In this section we develop a reduced complexity scheme based on the optimal scheme. We go backwards from (15) to (9) in the following steps:

1) Signal energy estimation assuming no interferers

Using only the first term in the sum in (15), we make an initial estimate $\hat{E}_{sv}=\langle E_{sv}|B^0E_vDI\rangle$ from

$$\begin{aligned} p(E_{sv}|B^0DI) &\propto p(E_{sv}|I)p(D|B^0E_{sv}DI) \\ &= p(E_{sv}|I)\prod_k p(R_k|B^0E_{sv}I) \end{aligned} \quad (16)$$

where the distributions $p(R_k|B^0E_{sv}I)$ are Gaussian with variance E_s+E_v, while $p(E_{sv}|I)\propto(E_s+E_v)^{-1}$. This leads to

$$p(E_{sv}|B^0DI)\propto\frac{1}{(E_s+E_v)^{N+1}}\exp\left(-\frac{\sum|R_k|^2}{E_s+E_v}\right). \quad (17)$$

This distribution is zero outside $[E_v+E_{s-}, E_v+E_{s+}]$, and its mean value is

$$\hat{E}_{sv} = \frac{\Gamma(N-1,b)-\Gamma(N-1,a)}{\Gamma(N,b)-\Gamma(N,a)}\sum_{k=0}^{N-1}|R_k|^2. \quad (18)$$

Here $a=\sum|R_k|^2/(E_v+E_{s-})$ and $b=\sum|R_k|^2/(E_v+E_{s+})$. Within the range of possible signal energies, the first factor in (18) is very close to $N-1$. This suggests

$$\hat{E}_{sv} = \frac{1}{N-1}\sum|R_k|^2 \quad (19)$$

as a reasonable approximation. Note that this estimate is based on the truth of B^0, so we are likely to be in large error if B^0 turns out to be false. This is the price we pay for reduced complexity.

2) Approximate marginalisation over all E_m

We perform the marginalisation involved in (14), for all m, by approximating the integral with a sum over discrete E_m, and replacing E_{sv} with $\hat{E}_{sv}$. Here we have a clear tradeoff between precision and complexity.

3) Channel classification and energy re-estimation

The posterior odds in (14) are computed and we introduce a threshold to classify channels as clear or interfered. We use this classification to re-estimate E_s without the contaminated data. For the first batch in each packet we also redo the marginalisation in step 2).

4) Interference energy estimation

By application of (12), (13), and the results from steps 2) and 3), we compute minimum mean square estimates $\hat{E}_m=\langle E_m|\hat{E}_{sv}D_mI\rangle$ for all channels classified as interfered.

5) Wiener smoothing with estimated signal energies

Finally, we use a Wiener smoother based on $\hat{E}_m$, $\hat{E}_s$ and E_v to estimate S_k. The integral in (10) collapses to

$$\hat{S}_k = \frac{\hat{E}_s}{\hat{E}_s + \hat{E}_m \sigma_{mk}^2 + E_v} R_k, \quad (20)$$

which basically is the smoother in (9). Go back to step 2) for the next batch in the packet.

For further reduction in computational complexity, we can use a subset of the data from each channel. For example, when estimating E_m we may use data from the frequency bins where most of the interferer energy is concentrated.

6 Suppression Performance

Simulations indicate that large performance improvements are obtainable with the proposed suppression scheme. In Figure 1 and Figure 2 we present results for the IEEE 802.11b rates 2 Mbit/s and 11 Mbit/s. Note that the packet error rates shown pertain to interfered transmissions. The actual rates are therefore not representative for a real situation, where not all packet transmissions are interfered.

The simulation code is available at *www.signal.uu.se*.

6.1 Simulation Parameters

The results reflect a constant flat fading environment and a signal-to-noise ratio of 15 dB. Batches are 256 samples ($\approx 23\ \mu$s).

A) IEEE 802.11b: Only the physical layer demodulation and symbol decoding is simulated, using perfect symbol synchronisation. The packets are 1500 bytes for 11 Mbit/s, 1024 bytes for 2 Mbit/s, containing pseudo-random data.

B) Bluetooth: The simulations include one, two or four interfering Bluetooth networks, hopping at 1600 Hz. In order to provide a severe test, all interferers are restricted to hop only within the receiver bandwidth. The given carrier-to-interference (CIR) ratios are with respect to the total interference power, which is distributed unevenly between the interferers. As suggested by [5], the transmit power is ramped up/down over 2 μs.

C) Reduced Complexity Implementation: The interferer energy E_m is quantised in steps of 1 dB. Out of the 46 bins per Bluetooth channel, only 10 are used in steps 5)-5) in the algorithm.

7 Conclusion

We have shown that a frequency domain approach using a Wiener smoother based on estimated signal energies is very effective in reducing Bluetooth induced packet errors. The gains are especially evident for the 2 Mbit/s rate.

The results, obtained with the reduced complexity approach without any tuning of the parameters, indicate that i) we can do even better by implementing of the full solution ii) we can achieve significant performance gains also when using more heavily reduced complexity. It should be kept in mind, however, that the results pertain to a flat fading environment and perfect synchronisation. The effects of interference on the synchronisation have not been taken into account, neither have the effects of fast fading.

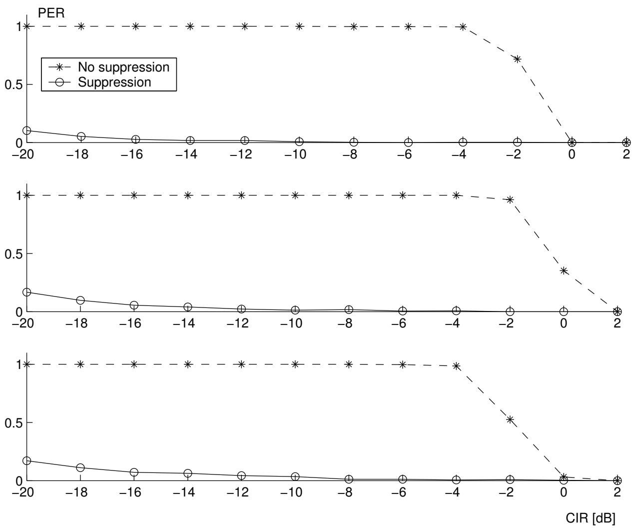

Fig. 1. Packet error rates (PER) for 2 Mbit/s rate. One interferer (top), two interferers (middle) and four interferers (bottom). Solid lines represent results with suppression, dashed lines without suppression.

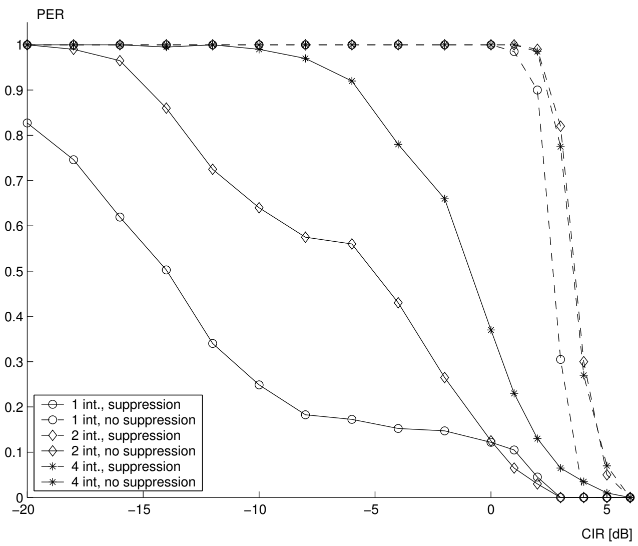

Fig. 2. Packet error rates (PER) for 11 Mbit/s rate. One interferer (circle), two interferers (diamond) and four interferers (star). Solid lines represent results with suppression, dashed lines without suppression.

References

[1] J. Lansford, A. Stephens and R. Nevo, "Wi-Fi (802.11b) and Bluetooth: Enabling Coexistence", *IEEE Network Mag.*, vol. 15, pp. 20-27, September-October 2001

[2] M. Fainberg and D. Goodman, "Analysis of the Interference Between IEEE 802.11b and Bluetooth Systems" *Proc. IEEE Vehicular Technology Conf.*, vol 2, pp. 967-971, October 2001

[3] C.F. Chiasserini and R.R. Rao, "Coexistence Mechanisms for Interference Mitigation in the 2.4-GHz ISM Band" *IEEE Trans. Wireless Commun.*, vol. 2, no. 5, pp. 964-975, September 2003

[4] Bluetooth Special Interest Group, *Specification of the Bluetooth System, Vol. 2, ver.1.2*, November 2003.

[5] A. Soltanian, R.E. van Dyck and O. Rebala, "Rejection of Bluetooth interference in 802.11 WLANs", *Proc. IEEE Vehicular Technology Conf.*, vol 2, pp. 932-936, September 2002

[6] E. T. Jaynes, *Probaility Theory – The Logic of Science*, Cambridge University Press, April 2003.

[7] IEEE Std 802.11, *Wireless LAN Medium Access Control (MAC) and Physical Layer (PHY) Specifications*, 1999 Edition